

# Optical Engineering

[OpticalEngineering.SPIEDigitalLibrary.org](http://OpticalEngineering.SPIEDigitalLibrary.org)

## **Photoelastic materials and methods for tissue biomechanics applications**

Rachel A. Tomlinson  
Zeike A. Taylor

# Photoelastic materials and methods for tissue biomechanics applications

Rachel A. Tomlinson<sup>a,\*</sup> and Zeike A. Taylor<sup>a,b,c</sup>

<sup>a</sup>The University of Sheffield, Department of Mechanical Engineering, Mappin Street, Sheffield S1 3JD, United Kingdom

<sup>b</sup>The University of Sheffield, CISTIB Centre for Computational Imaging and Simulation Technologies in Biomedicine, Mappin Street, Sheffield S1 3JD, United Kingdom

<sup>c</sup>The University of Sheffield, INSIGNEO Institute for in silico Medicine, Mappin Street, Sheffield S1 3JD, United Kingdom

**Abstract.** Digital photoelasticity offers enormous potential for the validation of computational models of biomedical soft tissue applications. The challenges of creating suitable birefringent surrogate materials are outlined. The recent progress made in the development of photoelastic materials and full-field, quantitative methods for biomechanics applications is illustrated with two complementary case studies: needle insertion and shaken baby syndrome. Initial experiments are described and the future exciting possibilities of using digital photoelasticity are discussed. © 2015 Society of Photo-Optical Instrumentation Engineers (SPIE) [DOI: 10.1117/1.OE.54.8.081208]

Keywords: tissue surrogate; birefringent; gelatine; konjac; needle insertion; shaken baby syndrome; biomechanics; model validation.  
Paper 150148SS received Feb. 3, 2015; accepted for publication Apr. 15, 2015; published online May 13, 2015.

## 1 Introduction

Advances in computational power have made feasible the modeling by engineers of highly complex human physiological systems, opening up a new level of engineering challenge. However, experimental validation of such models is obviously limited due to ethical issues. Physical models of these systems, using surrogate materials, provide an alternative means of validation, provided they, in turn, are reliable simulants of the real systems.

Photoelastic materials have been used for many years for visualization and analysis of strains in medical and dental applications, since many are mechanically similar to the relevant tissues. Birefringent materials, such as polymer resins, have been used to represent stiffer materials, such as bone and dentine, and gelatine, also known as ballistic gel, is often used as a surrogate to evaluate penetrating impacts or blast loading effects on soft tissues.<sup>1-4</sup> The use of photoelasticity for tissue analysis has been mainly limited to qualitative analysis since there are many issues that require consideration when developing flexible birefringent surrogate tissue materials for quantitative validation purposes. These include matching the modulus of elasticity to tissue types of different stiffness; transparency; modeling the viscoelasticity and creep observed in real tissues; representing the fibrous extracellular matrix (ECM) of tissue, particularly when punctured with medical instruments; and the stability of mechanical properties of surrogate materials over time and at different temperatures. Lower modulus photoelastic materials are also of interest in non-“bio” applications, such as in the work of Dubey and Grewal,<sup>5</sup> yet even in latter work, the involved material had a stiffness of ~4 MPa, which is still several orders of magnitude higher than that of many soft tissues.

In addition to the complications of creating suitable surrogate materials, the complex three-dimensional (3-D) nature

of biological load systems adds challenges to strain analysis. Many experimental strain analysis techniques, such as digital image correlation, thermoelastic stress analysis, or electronic speckle pattern interferometry,<sup>6</sup> make surface measurements only. Others such as neutron and x-ray techniques can map internal structures but require expensive equipment. Stress-freezing photoelasticity is well established as a technique that can evaluate internal strains in scale models of 3-D load systems.<sup>7</sup> This method requires a polymer model to be loaded and subjected to a thermal cycle to lock in strains. The model is then sectioned to allow two-dimensional (2-D) analysis, which is necessary due to the integral nature of the method, but also destroys the model. However, other non-destructive, automated tomographic and integrated photoelasticity techniques<sup>8</sup> have the potential to allow live-loading and real-time analysis of 3-D photoelastic models of flexible biological systems, aided by the recent rapid development of fast computing and higher-resolution cameras.

This paper will consider the progress made in the development of photoelastic materials and full-field, quantitative methods for biomechanics applications and will be illustrated with two complementary case studies: needle insertion and shaken baby syndrome (SBS). Both of these research projects are in their infancy and are presented here to highlight the potential of digital photoelasticity for biomedical applications.

### 1.1 Background to the Development of Soft Photoelastic Materials for Biomechanical Applications

Needle insertion is a common surgical procedure used in everything from drug administration to biopsy extraction. Many such applications would benefit from robust and flexible numerical models of the needle insertion process. For example, during a biopsy procedure, the hollow needle, usually with a notch near the tip, can be guided with the aid of

\*Address all correspondence to: Rachel A. Tomlinson, Email: [r.a.tomlinson@sheffield.ac.uk](mailto:r.a.tomlinson@sheffield.ac.uk)

ultrasound to cut and retrieve small tissue samples from the body. Guidance problems may arise when the targeted area is deep in the body, requiring a relatively large distance to be traveled by the needle tip. Also, the tip of the needle is not symmetrical, so forces acting on the tip will be uneven, consequently resulting in bending of the needle in the body during insertion.<sup>9,10</sup> The bending can cause inaccuracy in the needle placement, and consequently, the needle tip may miss pathological tissue and result in misdiagnosis.<sup>11</sup> Additionally, if one considers small breast lesions, for example, during biopsy the target may move significantly as the needle indents and punctures the skin and successive tissue layers.<sup>12</sup> The target may penetrate deeper into the breast soft tissue, making it more difficult for the needle to reach the lesion. Therefore, this case study aims to explore the strains due to tissue–needle interaction in order, ultimately, to improve the reliability of needle placement within a body by predicting tissue and needle deflections.

SBS is a result of physical child abuse that leads to the deaths of ~200 infants in the United Kingdom every year.<sup>13</sup> Previous academic work from a biomechanical perspective has been largely unable to explain the kind of injuries observed from cases of suspected SBS, with an influential study by Duhaime et al.<sup>14</sup> hypothesizing that most suspected SBS injuries could not be caused by shaking alone. Misdiagnosis can have huge social ramifications for the families involved. False positives can cause unjust loss of custody of the baby and criminal sanctions, while false negatives could delay treatment and allow the baby to remain at risk of further abuse and injury.<sup>15</sup> If the modes and magnitudes of the strain placed on an infant's brain during a shaking event are known across the full field of the brain, a better understanding of how injury occurs could be developed. This research aims to investigate the strains experienced by the brain tissue by using simplified physical models of an infant's skull and involves dynamic loading within a polariscope.

## 2 Development of a Surrogate Tissue Material

The first step of the development of a surrogate material is to investigate the mechanical properties of human tissue. If we consider needle biopsies, the procedures and tools used are normally similar on all patients, but the mechanical properties of tissue vary according to gender and age group.<sup>16</sup> Also, the characteristic of each layer of tissue may have to be considered. For example, in a breast cancer biopsy, upon puncturing the skin, the needle may pierce layers of fat, glandular tissue, and muscles.

Saraf et al.<sup>17</sup> performed experiments on four types of soft tissue: stomach, liver, heart, and lung. The tissues were put under hydrostatic compression and simple shear to obtain the dynamic response. Their study concluded that the tangent shearing moduli of the four tissues range from 0.008 to 0.34 MPa. In terms of shearing, the liver tissue was found to be stiffest while the lung tissue was the softest. However, the dynamic bulk moduli vary from 150 to 500 MPa, with the stomach being the stiffest and the lung, again, the softest. In addition, it is widely recognized that these and most other soft tissues do not exhibit linear elastic behavior, meaning such results are approximations only.

In a study by Davis et al.,<sup>18</sup> the force required to insert a micro-needle into living skin was measured and found to depend heavily on the sharpness and size of the needle, but that as the needle punctured the tissue, the fracture toughness could affect the overall strength of the tissue. Taylor et al.<sup>19</sup> found skin fracture toughness values to be highly variable and strongly dependent on the crack growth. They found that specimen size was important since stress and failure energy were seen to be constant for larger specimens with no dependence on crack size. Furthermore, it is of interest that soft tissues were found to be highly tolerant to defects as they could withstand cracks up to several millimeters without losing much strength.

The mechanical properties of brain tissue are complex, nonlinear, and time dependent. For example, in a study by Miller et al.,<sup>20</sup> a probe was inserted into the brain of a swine while under anesthesia. The probe was fitted with a strain-gauge load cell. The results from this were then compared to a finite element study using a linear-viscoelastic solution, but this was found to have poor accuracy when compared to experimental results.

All of these results demonstrate that the mechanical responses of soft tissues are highly variable between tissue types and even between locations within individual organs, but that all are nonlinear, most show time and strain rate dependence, and many show resistance to tearing. Since the present work was undertaken from an engineering point of view, we aimed to keep candidate surrogate materials as simple as possible, concentrating on ease of use, availability, and cost. A range of materials were tested as potential surrogates, considering (1) resistance to tearing when punctured; (2) response under load; and (3) transparency and birefringence. The materials considered were gelatine, gelatine with additives, konjac, and agar.

Gelatin-based materials are commonly used to represent soft tissues, and several studies have been performed to characterize their mechanical properties.<sup>1,2</sup> The work by Kwon and Subhash<sup>2</sup> shows that 11% concentrated gelatine results in a Young's modulus of 10.9 kPa. Their experiment focused on the strain rate sensitivity of the gelatine and different responses were obtained under different loading conditions. Gelatine concentrations of 5, 7, and 14% yielded average Young's moduli of 40, 63, and 110 kPa, respectively.<sup>3</sup> The difference in stiffness between these two studies might be due to the types of raw gelatine powder used. Kwon and Subhash<sup>2</sup> used engineering gelatine powder with a known Bloom strength of 250, while Markidou et al.<sup>3</sup> used gelatine powder for food preparation. The latter has a lower Bloom strength and is expected to have a value of ~60 to 80. The Bloom level is a measure of toughness; therefore, higher Bloom value gelatines are more resistive to tearing. Glycerol and sorbitol have been added to gelatine mixtures, where glycerol acts as a plasticizer that increases the molecular weight.<sup>4</sup> Different ratios of glycerol and sorbitol were mixed together with gelatine, and it was found that an increase in the proportion of glycerol caused an increase in flexibility, but the material suffers an overall loss in strength.

In our initial experiments, a mixture only consisting of gelatine powder and water was used. 20 g of gelatine powder for food preparation was mixed with 200 ml water for a 1 : 10 ratio and refrigerated (5°C) overnight. Leaving the mixture

**Table 1** Composition, photoelastic fringe constant, and Young's modulus of the gelatine specimens.

Specimens	Composition	Fringe constant, $f$ (N/m fringe)	Compressive modulus, $E$ (kPa)
Gelatine:Water	1:10	36	27.3
	2:10	33	56.9
	3:10	28	84.1
Gelatine:Water:Glycerin	2:10:10	82	47.5
	3:10:10	85	75.5
	3:5:10	115	112.5
Gelatine:Glycerin:Sorbitol	4:10:10	152	120.6

overnight allows proper blooming of the gelatine and also means the gelatine crystals have enough time to absorb liquid. The blooming process is very important as it ensures the smooth texture of the finished product. After leaving it overnight, the gelatine mixture crystallized and the grains could be seen to have enlarged. The cluster of gelatine grains were then heated to  $\sim 60$  to  $70^\circ\text{C}$ , taking care not to let the mixture boil as this introduces bubbles. Once the mixture was fully liquefied, it was poured into the cylindrical mold and cooled to room temperature. The cooled mixture was then refrigerated overnight again before testing to ensure that it was completely set.

A similar procedure was used with different ratios of gelatine to water, and with additives of glycerin and/or sorbitol as indicated in Table 1. An attempt was made using a systematic process to fabricate usable specimens at the highest concentration possible, but which would still solidify. Only one composition of gelatine powder, glycerin, and sorbitol (4:10:10) was successful because the nature of the substances made it difficult for the gelatine powder to absorb. Hence, the blooming period was extended to three days for the mixtures with additives, to allow the gelatine to crystallize fully.

The konjac gel is derived from the konjac plant and is commonly known in Asia as "Konnyaku." It was considered that the fibrous microstructure of the konjac might provide superior fracture toughness over gelatine. To fabricate, konjac powder (since this product is for culinary purposes, there is considerable variability between different brands; Jim Willie Konnyaku Jelly Powder was used here) was mixed with sugar and then gradually added to boiling water while stirring gently to ensure even mixing. The mixture was poured into a mold and cooled to room temperature before setting in the refrigerator overnight. Different ratios of konjac, water, and glycerin were analyzed (Table 2).

Agar is derived from algae and is used as a culinary thickening agent, growth medium for bacteria in science labs, and a dental impression material. It was supplied in a solid gel form, so it was heated gently until it turned liquid and then was poured into the mold and cooled to room temperature before leaving it to re-set in the refrigerator overnight.

**Table 2** Composition of konjac jelly test specimens.

Mixture	Specimens	Composition	Comments
A	Konjac:Water	1:10:75	Sags more than C
B		1:10:50	Sags more than C
C		1:10:30	Final choice
D	Konjac:Water:Glycerin	1:10:20:10	Too viscous
E		1:10:0:30	Very low stiffness

## 2.1 Resistance to Tearing When Punctured

The needles used in our experiments were scaled-up models made from 5-mm-diameter steel rods.

Figure 1 shows a 45-deg bevel needle inserted into each material. The fibrous nature of the konjac may be seen to afford it greater resistance to tearing than the gelatine or the agar. The konjac clings to the needle as it is inserted [Fig. 1(b)], whereas the surfaces of the gelatine and agar split, forming a tear [Figs. 1(c) and 1(d)]. The agar performed no better than the gelatine under the tearing test and was discounted, since the gelatine was a more established surrogate material.

## 2.2 Response Under Load

A cylinder sample (diameter = 50 mm, approximate height = 70 mm) of each gelatine material was loaded in compression in a Tinius Olsen 5 kN single column H5kS benchtop test machine with a step increment of 1 mm displacement, starting from 0 to 10 mm displacement, while its corresponding reaction force was recorded. The tests were repeated three times for each specimen and the compressive modulus was determined (Table 1). Due to the barrelling effect under load, the stress was calculated from the load using an average area with consideration of the constant volume.<sup>21</sup> The stress-strain response was approximately linear as shown in Fig. 2(a) for the gelatine with additives.

A similar procedure was performed with the konjac specimens. Figure 2(b) shows an example of the data recorded using mixture C at a strain rate of 5% of the gauge length per second during three cycles of loading and unloading. The behavior was highly nonlinear and showed distinct hysteresis (referred to as conditioning in the tissue biomechanics literature). From the point of view of the material's use as a tissue surrogate, these are interesting phenomena given the characteristics of soft tissues described above.

## 2.3 Transparency and Birefringence

Specimens of similar dimensions ( $\sim 50$  mm diameter, 30 mm thickness) of the konjac and gelatine were loaded in diametral compression in a circular polariscope. Figure 3 shows the birefringent response of konjac (mixture C) and gelatine (composition 3:10:10). Both materials were birefringent, but the konjac possessed poor optical properties and it is postulated that this is the result of scattering within the fibrous material. The gelatine possessed better optical and

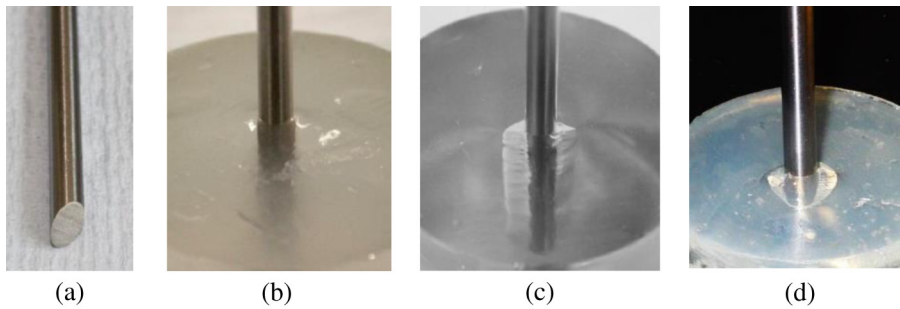


**Fig. 1** (a) 45-deg bevel needle inserted into (b) konjac gel, (c) gelatin, and (d) agar. The konjac clings to the needle, whereas the gelatine and agar tear.

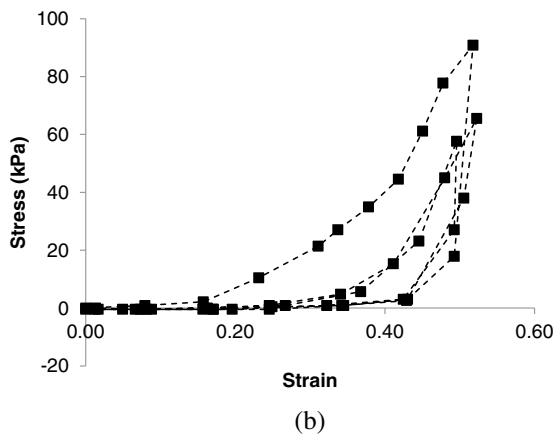
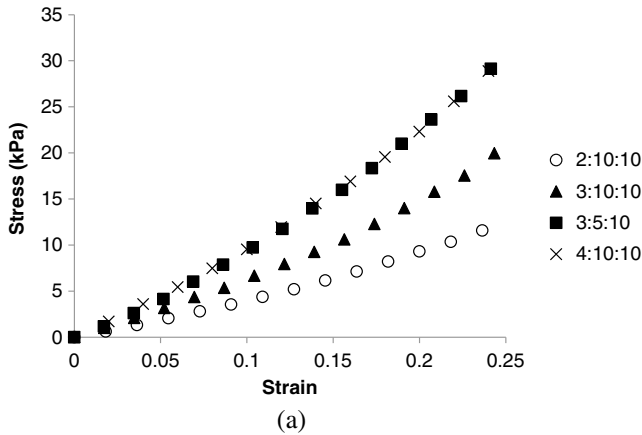


**Fig. 2** Stress-strain response of (a) gelatine (with additives, Table 1) and (b) konjac (mixture C). Results of three loading and unloading cycles are shown for the konjac.

birefringent properties, therefore, a standard disc in diametral compression calibration test<sup>22</sup> was performed to determine the photoelastic fringe constant,  $f$ , for the different mixtures of gelatine. The results are presented in Table 1 and show that the highest fringe constant was achieved by the mixture containing both glycerin and sorbitol.

The viscoelastic properties of the konjac jelly adds complexity to the determination of optical properties, which will be discussed later.

### 3 Case Studies

From the results of the surrogate material experiments, it could be argued that gelatine is the most suitable option for biomedical photoelasticity tests; of the materials tested, it had the best transparency and birefringent sensitivity, and the modulus can be varied with the use of additives to represent the varying stiffness of the human body. The lower stiffness specimen (2:10:10) could represent soft tissues, such as the stomach or lung, and the stiffer gelatine (3:5:10) could simulate the heart or liver.<sup>17</sup> The konjac showed excellent resistance to tearing when compared to the gelatine and agar (Fig. 1), but the transparency was poor (Fig. 3). It also showed a strongly non-linear and hysteretic response, which is more representative of human tissue than the weakly non-linear and elastic behavior of the gelatine (Fig. 2).

The photoelastic calibration shows that the concentration of gelatine and additives directly affects the fringe constant. While the specimen with added sorbitol produced the highest fringe constant, this was not a significant increase compared to the mixture with glycerin only.

For the first experiment, the 3:10:10 gelatine was selected as it exhibits repeatability in mechanical and

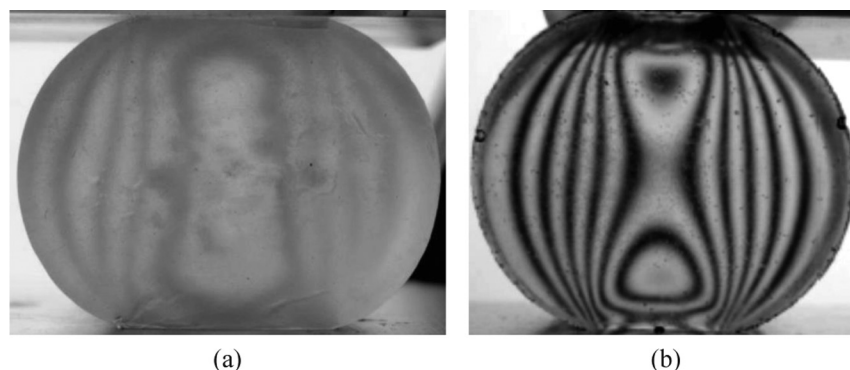


**Fig. 3** Birefringence of (a) konjac gel and (b) gelatine.

photoelastic properties with an acceptable toughness and the ratio is the most appropriate to emulate aged human skin.

### 3.1 Puncture Experiment

A new set of gelatine-glycerin-water specimens (mixture 3:10:10) was prepared for a puncture experiment. A scale model of a 25-deg bevel tip needle (Westcott) was made from a 5-mm-diameter steel rod and was attached to a Tinius Olsen machine, was placed just touching the gelatine specimen, and the load cell and displacement readings were both set to zero. The needle was then displaced and every 0.5 mm its corresponding reaction force was recorded. Photoelastic images were recorded in a light field circular polariscope at intervals of displacement and are shown with the force-displacement curve in Fig. 4(a). Figure 4(b) shows the photoelastic response as the needle is inserted further into the gelatine.

Figure 4(a) shows a steady force increase with displacement, which drops abruptly at 3 mm, indicating the puncture event. At this point, the first crack is initiated and the accumulated strain energy is relaxed, resulting in a sharp drop in force. Following penetration, there is a saw-tooth pattern corresponding to incremental insertion steps of 0.5 mm, followed by short pauses where data were recorded and in which the force relaxes. The cutting and elastic deformation force components are similar in each increment, and the

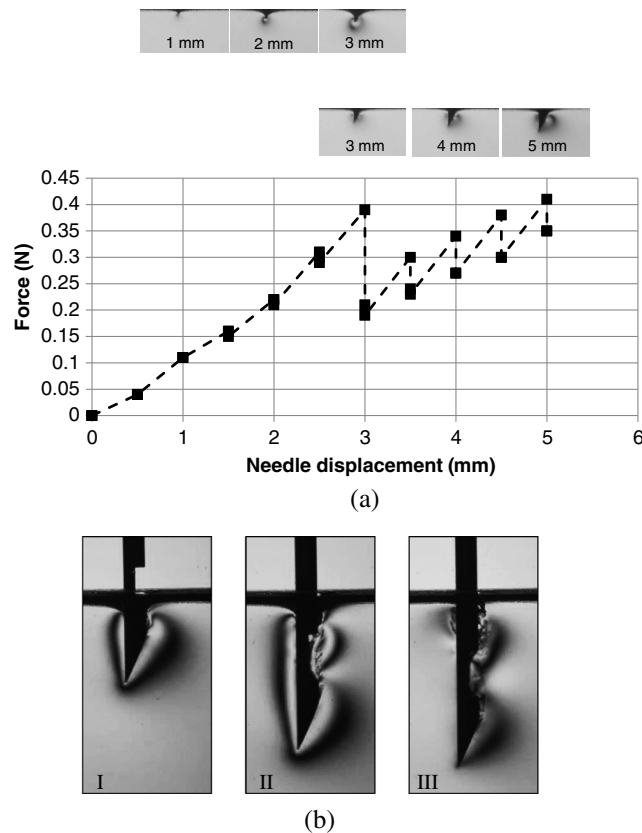


**Fig. 4** (a) Force-displacement response of 25-deg bevel needle tip in the 3:10:10 gelatine specimen and the corresponding photoelastic images in a light field circular polariscope, before (upper row) and after (lower row) penetration. (b) Photoelastic images as the needle is inserted in the gelatine (I and II) and the relaxation of fringes as the needle is held stationary (III).

overall increase is due to higher friction as more of the needle shaft enters the specimen.

The corresponding fringe patterns add more information. Before the puncture, the photoelastic fringe, which represents the maximum shear stress, can be seen to surround the tip uniformly, but after the material had been punctured, the accumulated stresses at the tip were relieved. Then as the needle was inserted, the fringe growth showed an increase in shearing force, and the hypothesis of an asymmetric force distribution on bevel tipped needles was also confirmed.

During needle insertion, the reaction force on the needle is the sum of contributions from tissue rupture ahead of the tip, tissue deformation in the vicinity, and friction between the tissue and needle (see also the detailed discussion in Ref. 23). Furthermore, any change in geometry along the needle will also cause changes in the needle-tissue response. For example, the work required to puncture the skin is much higher than the work required to cut the tissue due to the high stress concentration on the crack tip. Therefore, the insertion of the needle cannot be considered as a single motion. The needle insertion process can be separated into three phases, which are the deflection on skin before puncture, insertion of the needle tip, and insertion of the tip and shaft.

Due to the tissue's elasticity, the needle does not puncture the tissue upon contact but instead the compliant tissue boundary moves with the needle. The small area where the needle pushes the boundary is called the interfacial area. The small interfacial area creates high stress levels with minimal force, until eventually a crack is initiated.

Following the initial point of penetration, a rupture often propagates rapidly because the large amount of strain energy stored during the boundary displacement phase is released at once to extend the rupture. As a result, a large drop in force is noticed and the subsequent cutting forces can be seen to be lower than the initial puncture force, due to the presence of the crack. However, additional puncture events may occur as the needle pierces further into the tissue due to tissue inhomogeneity. Additionally, the insertion force also includes the effort to push the crack apart caused by the gradual increase of contact area of the bevel needle tip. Hence, the increase in force is nonlinear at this stage.

As the needle is inserted further [Fig. 4(b)], the needle tip is still subjected to a cutting and/or puncture force, but the behavior is much more consistent as the interfacial area of tip and tissue remains constant.<sup>24</sup> The increasing contact area between the shaft and the tissue causes increasing friction force throughout the insertion process. Although most of the stock needles manufactured are lubricated, some friction inevitably persists. In Fig. 4(b), the fringe on the left of the needle is only observed when the needle is moving (I and II), but when the needle stops (III), this fringe disappears; therefore, it may be deduced that this fringe is due to the friction force applied. As the force is removed, the fringes due to friction relax.

### 3.2 Shaken Baby Syndrome Experiment

Attempting to model the 3-D complexity of the skull was deemed too ambitious for an initial experiment; therefore, a simplified 2-D model was manufactured as shown in Fig. 5.

The model consists of an acrylic cylinder to represent the cranium, with a plastic insert as the brain stem. Foam inserts were fitted as shown and mold release gel was used to ensure

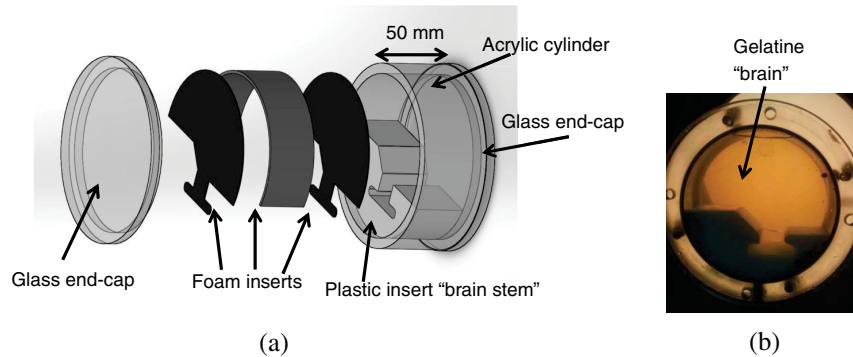


**Fig. 5** (a) Assembly of two-dimensional brain model mold and (b) gelatine brain in the mold.

that the inserts could be removed without sticking. The gelatine solution was poured in and left to set at 3°C for 18 h. After the solution had set, the inserts were gently removed with tweezers and the optical qualities of the gelatine inspected using a polariscope [Fig. 5(b)]. The voids from the inserts were filled with cold water at 3°C to represent the cerebrospinal fluid and the stress-free glass end caps were closed securely. It was important to ensure that the gelatine specimen was fully surrounded by a water film to enable free movement. If movement was restricted, the stress pattern would be an integral of the dynamic stresses plus sticking stresses.

A study by Miller et al.<sup>20</sup> concluded that, excluding time-dependent effects, a modulus value of 50 kPa was a reasonable estimate for brain tissue in compression, so an initial gelatine:water formulation of 2:10 was chosen (Table 1). It should be noted that other studies have used lower moduli but of the same order of magnitude.<sup>13</sup>

The shaker rig was a purpose built structure using a pneumatic actuator that can oscillate the specimen with different levels of acceleration and amplitude, replicating those measured from shaking a crash test dummy. The rig was adapted from the system used by Cheng et al. and further details may be found in their paper.<sup>13</sup> The rig was assembled inside a circular polariscope as in Fig. 6.

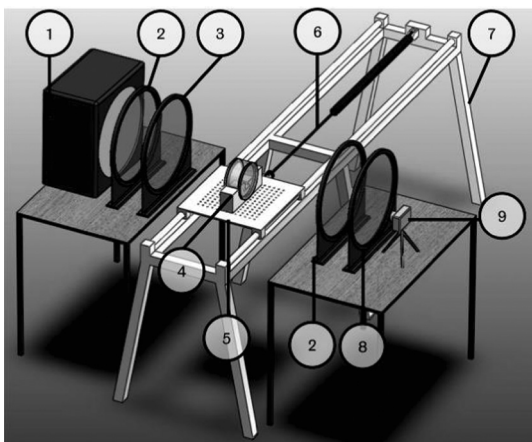


**Fig. 6** Shaker rig in the polariscope: (1) sodium light source; (2) quarter wave plate (x2); (3) polarizer; (4) acrylic cylinder (containing gelatine brain); (5) shaker tray; (6) pneumatic actuator (max. pressure 6 bar); (7) shaker rig structure; (8) analyzer; (9) camera.

A video recording was made while the shaker rig oscillated the specimen. The recorded video was then split into individual frames, which could be processed to determine fringe order and hence internal stresses.

Figure 7 displays a sequence of six frames showing the maximum shear strain in the brain under dynamic loading (equivalent to one tenth of a second of motion). Frame i shows the specimen entering the frame from the left, decelerating as it travels. By frame iv, the velocity is approximately equal to zero. This also represents the point of maximum acceleration. By frame vi, the specimen's velocity is increasing and it is exiting to the left of the frame. The fringe patterns on the specimen change over time as the specimen's acceleration changes, reaching a peak fringe density on frame iv at the point of maximum acceleration.

The stress maps indicate peak values in the brain stem area, with the maximum shear stress peaking at 1150 Pa in frame iv. However, this peak stress remains in frames v and vi, even though the acceleration is decreasing. So the maximum shear stress is lagging slightly behind peak accelerations, in agreement with observations by Couper and Albermani.<sup>25</sup>

The results of this study appear to agree with the Duhaime hypothesis,<sup>14</sup> which states that the injuries seen in infants with a case of suspected SBS cannot be accounted for by shaking alone, as the forces are too low for trauma within the brain tissue, and the injuries are instead caused by an additional event, such as an impact. This study mirrors such findings as the maximum shear stresses measured experimentally peak at slightly over 1 kPa, which is well below the 20 kPa typically required for permanent brain damage to occur. However, this is a very simplified model and further work is clearly required for more conclusive results.

### 3.3 Deficiencies of the Experiments

The needle and SBS experiments demonstrate the enormous potential of using photoelasticity for soft tissue analysis; however, there are drawbacks to overcome. Although the gelatine exhibits excellent birefringent properties and its stiffness may be tailored to approximate different tissues, other tissue characteristics are not emulated by this material. For example, the fibrous ECM of tissue is not well represented by the granular microstructure of gelatine, which tears easily. Nor does it appear to exhibit time dependence and hysteresis as strongly as do real tissues. Moreover, the

two experiments performed are only semiquantitative since they only record (half) integer fringes at increments of the load. Digital photoelasticity, by contrast, has the potential to record full-field quantitative data in near-real-time. Therefore, a second set of experiments was conducted using more advanced techniques.

### 3.4 Application of Digital Photoelasticity

#### 3.4.1 Needle insertion using phase-stepping photoelasticity

Since it was found that the konjac has the potential to more accurately replicate the time-dependent and puncture properties of tissue, the needle insertion experiment was repeated using the konjac as the surrogate material. For each load step, six phase-stepped images were recorded sequentially following the method proposed by Siegmund et al.<sup>26</sup> Figure 8 shows the initial results: the full-field isochromatic and isoclinic data. It may be observed that there is some minor data loss in the isochromatic map due to the isoclinic being undefined at half-order fringes. Also, unwrapping the periodic function close to the needle introduced some noise, but this can be overcome by using a higher-resolution camera.

While the poor optical properties of the konjac make its use in traditional photoelasticity difficult, the results above demonstrate that it is viable in the case of digital photoelasticity. This is particularly beneficial for studying the mechanics of needle/tissue interactions given the close emulation of

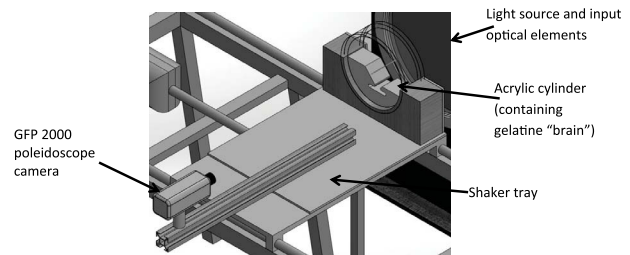


**Fig. 9** Experimental arrangement of the shaken baby syndrome experiment using the GFP 2000.

tissue elastic and rupture behavior that the konjac appears to offer. The strain fields in the vicinity of the needle tip identified by this means are correspondingly more likely to be indicative of those in real tissues.

#### 3.4.2 SBS experiment using a poleidoscope

To enable digital photoelastic analysis of the dynamic shaking event, a GFP 2000 Poleidoscope (Stress Photonics Inc.)<sup>27</sup> was employed. This instrument has an objective lens that splits the image into four parts, each image having different optical elements to allow phase-stepped photoelastic images to be captured in one frame. Therefore, digital photoelasticity may be performed on moving objects, as in the case of the SBS experiment.

The output elements of the polariscope (2, 8, and 9 in Fig. 6) were replaced by the poleidoscope system mounted

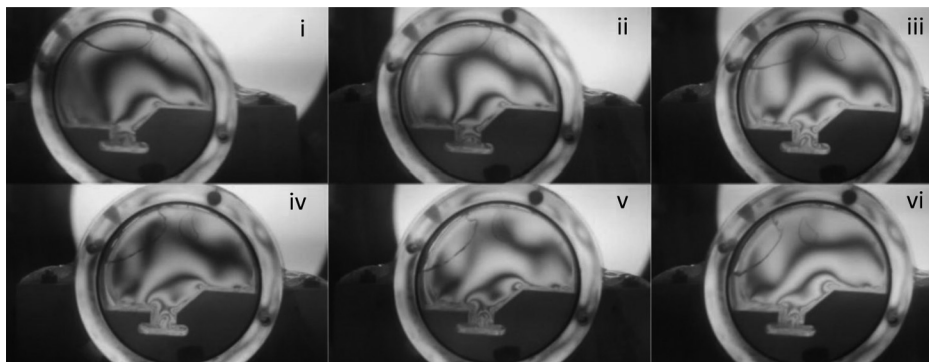


**Fig. 7** Photoelastic fringe patterns in the brain during a period of acceleration (max 3g). The time between each frame is 17 ms.

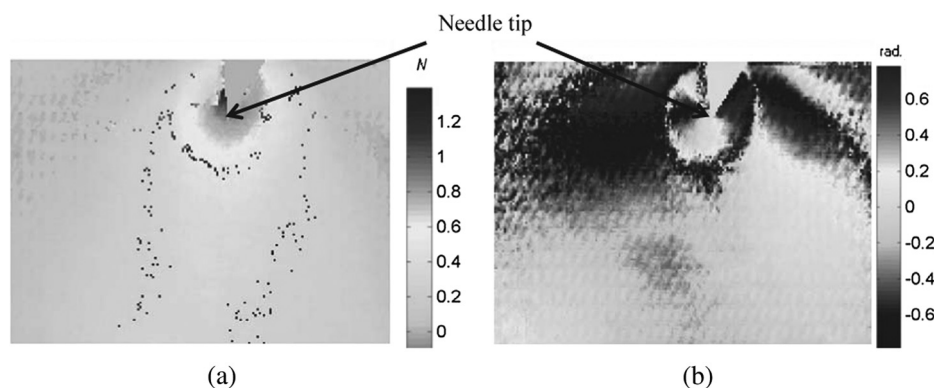


**Fig. 8** Full-field (a) isochromatic and (b) isoclinic data around the tip of a 25-deg bevel needle tip inserted into konjac.

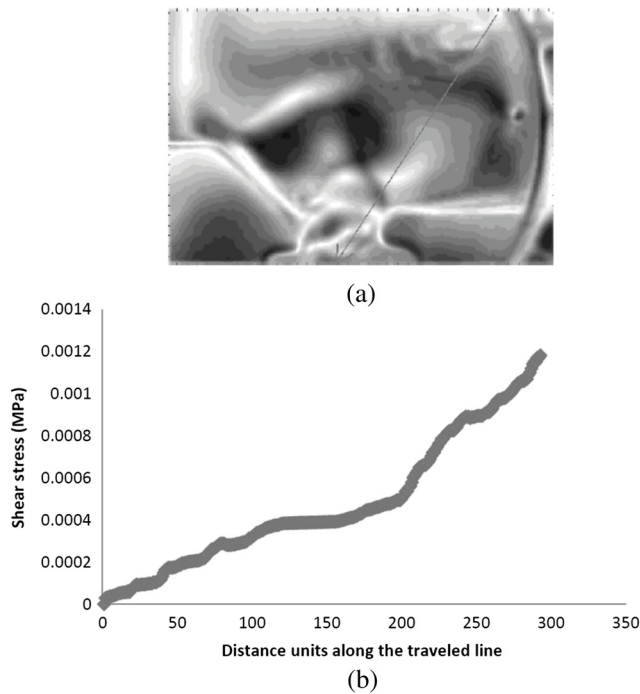


**Fig. 10** (a) Map of maximum shear stress of the bottom right section of the brain for one oscillation at maximum acceleration to the left and (b) plot of the maximum shear stress along the line indicated in (a).

on the shaker tray as in Fig. 9. The brain was shaken with a maximum acceleration of 7.2g. This compares to a maximum of 10g that has been recorded in shaking tests on anthropomorphic dummies of infants.<sup>28</sup> Figure 10 displays the brain stem area of the specimen, which recorded the maximum shear stress of 1180 Pa.

#### 4 Discussion and Conclusion

This work is still in preliminary stages and further research is needed to develop a robust full-field experimental method for validating computational models of needle insertion and SBS. Although the gelatine mixed with glycerin was used for the photoelastic tests and showed good optical properties and controllable stiffness, its tearing characteristics are quite different from those of biological tissues. On the other hand, the mechanical properties of konjac, both in terms of stress-strain and tearing behavior, are very similar to those of biological tissues, yet its optical properties are clearly inferior. Experiments are underway to quantify further its constitutive behavior for more detailed comparison with those of tissues. It is also acknowledged that the mechanical isotropy of the presented surrogate materials makes them simpler in this respect than most real tissues which usually exhibit some degree of anisotropy. Nonetheless, these materials constitute a starting point for a much wider research program, which potentially will involve engineering the chemistry of polymer materials for soft tissue photoelasticity similar to work already carried out for mechanical analysis of polymer gels for defense applications.<sup>29</sup>

Another factor not discussed in this work is the influence of the insertion force magnitude and the insertion rate on the magnitude of needle deflection. Besides the cutting force, the shearing caused by friction between the needle shaft and the tissue is also damaging to the material. Since

photoelasticity provides a map of maximum shear strain, the technique appears ideal for investigation of friction.

Photoelasticity is by no means limited to use on simple, linearly elastic materials. Another branch of theory exists called photoviscoelasticity, and experiments have been conducted on materials with significant viscoelastic effects, such as epoxy resin with excessive plasticizer in a study by Zhao and Huang.<sup>30</sup> In their particular experiment, the material is still quite rigid and the viscoelastic effects studied are related to the material failing after strain builds up over time; it is plausible, however, that with further research this theory could be applied to soft materials, such as a tissue surrogate. Due to the complexities of the theory,<sup>31,32</sup> a full photoviscoelastic study was not attempted in this project, but it is potentially a means of validating even time-dependent models of needle-tissue interaction should this be desired.

As discussed, soft tissues have a range of material properties that are highly dependent on age, function, temperature, etc., so any value determined from *in vivo* or *ex vivo* experiments will involve a degree of uncertainty. Computational modeling has a great advantage over physical modeling in that properties may be easily changed, but these models must still be validated in some way. One proposal is to develop a simplified physical model that adequately simulates the human function and properties and then construct a numerical model of that system. If the numerical model is validated by the physical surrogate, then confidence is gained in the computational procedure, which can then be developed for more complex, biologically accurate systems.

The 3-D nature of biological systems adds complexity to this research. In this research, we have started with simplified 2-D physical models and demonstrated the potential of dynamic digital photoelasticity. But for 3-D analysis, the integral nature of photoelasticity is a challenge, especially when combined with the dynamic nature of the problems presented and the strain rate dependency of the materials. Scalar medical tomographic techniques currently require the patient to remain still throughout the scanning procedure, so tensor tomography on dynamic systems is a huge engineering challenge. One solution would be to utilize the versatility of computational methods. In their work on streaming birefringence, Spalton et al.<sup>33</sup> performed a 3-D experiment and recorded integrated photoelastic data. The 3-D simulation data were validated by the experiment by manipulating the computational data to simulate the integral effect. The authors believe that a similar use of hybrid experimental-computational methods, using the respective advantages of both approaches with new birefringent materials and modern digital photoelasticity, offers exciting possibilities for analyzing highly complex human physiological systems.

#### Acknowledgments

The authors would like to gratefully acknowledge the experimental contributions of Wei Kang Aui Yong, Guy Morton, Jasper Roseland, and Ling Wei Yap, and also would like to thank VisEng Ltd. for the loan of the GFP 2000 Poleidoscope.

#### References

1. D. S. Cronin and C. Falzon, "Characterization of 10% ballistic gelatin to evaluate temperature, aging and strain rate effects," *Exp. Mech.* **51**, 1197–1206 (2011).

2. J. Kwon and G. Subhash, "Compressive strain rate sensitivity of ballistic gelatin," *J. Biomech.* **43**(3), 420–425 (2010).
3. A. Markidou, W. Y. Shih, and W. Shih, "Soft-materials elastic and shear moduli measurement using piezoelectric cantilevers," *Rev. Sci. Instrum.* **76**(6), 064302 (2005).
4. M. Thomazine, R. A. Carvalho, and P. J. A. Sobral, "Physical properties of gelatine films plasticized by blends of glycerol and sorbitol," *J. Food Sci.* **70**(3), E172–E176 (2005).
5. V. N. Dubey and G. S. Grewal, "Efficacy of photoelasticity for developing whole-field imaging sensors," *Opt. Lasers Eng.* **48**(3), 288–294 (2010).
6. W. N. Sharpe, Ed., *Springer Handbook of Experimental Solid Mechanics*, Springer Science+Business Media, LLC, New York (2008).
7. H. Fessler, "An assessment of frozen stress photoelasticity," *J. Strain Anal.* **27**(3), 123–126 (1992).
8. H. Aben, *Integrated Photoelasticity*, McGraw Hill, New York (1993).
9. A. Jahya, F. van der Heijden, and S. Misra, "Observations of three-dimensional needle deflection during insertion into soft tissue," in *Int. Conf. Biomedical Robotics and Biomechatronics*, pp. 1205–1210 (2012).
10. N. Abolhassani, R. Patel, and M. Moallem, "Needle insertion into soft tissue: a survey," *Med. Eng. Phys.* **29**, 413–431 (2007).
11. S. Misra et al., "Needle-tissue interaction forces for bevel-tip steerable needles," in *IEEE RAS & EMBS Int. Conf. on Biomedical Robotics and Biomechatronics*, pp. 224–231 (2008).
12. M. Abayazid et al., "Effect of skin thickness on target motion during needle insertion into soft-tissue phantoms," in *Fourth IEEE RAS/EMBS Int. Conf. on Biomedical Robotics and Biomechatronics*, pp. 755–760 (2012).
13. J. Cheng, I. C. Howard, and M. Rennison, "Study of an infant brain subjected to periodic motion via a custom experimental apparatus design and finite element modelling," *J. Biomech.* **43**(15), 2887–2896 (2010).
14. A. C. Duhaime et al., "The shaken baby syndrome: a clinical, pathological and biomechanical study," *J. Neurosurg.* **66**, 409–415 (1987).
15. C. Jenny et al., "Analysis of missed cases of abusive head trauma," *J. Am. Med. Assoc.* **281**(7), 621–626 (1999).
16. Y. Zheng and A. F. Mak, "Effective elastic properties for lower limb soft tissues from manual indentation experiment," *IEEE Trans. Rehabil. Eng.* **7**(3), 257–267 (1999).
17. H. Saraf et al., "Mechanical properties of soft human tissues under dynamic loading," *J. Biomech.* **40**(9), 1960–1967 (2007).
18. S. P. Davis et al., "Insertion of microneedles into skin," *J. Biomech.* **37**, 1155–1163 (2004).
19. D. Taylor et al., "The fracture toughness of soft tissues," *J. Mech. Behav. Biomed. Mater.* **6**, 139–147 (2012).
20. K. Miller et al., "Mechanical properties of brain tissue *in-vivo*: experiment and computer simulation," *J. Biomech.* **33**(11), 1369–1376 (2000).
21. P. P. Benham, R. J. Crawford, and C. G. Armstrong, *Mechanics of Engineering Materials*, p. 497, Addison Wesley Longman Ltd., Harlow, Essex (1996).
22. G. Cloud, *Optical Methods of Engineering Analysis*, Cambridge University Press, Cambridge, UK (1995).
23. N. Vaughan et al., "A review of epidural simulators: where are we today?" *Med. Eng. Phys.* **35**(9), 1235–1250 (2013).
24. D. J. van Gerwen, J. Dankelman, and J. J. van den Dobbelsteen, "Needle-tissue interaction forces: a survey of experimental data," *Med. Eng. Phys.* **34**, 665–680 (2012).
25. Z. Couper and F. Albermani "Mechanical response of infant brain to manually inflicted shaking," *J. Eng. Med.* **224**(H1), 1–15 (2010).
26. P. Siegmann, D. Backman, and E. A. Patterson, "A robust demodulation and unwrapping approach for phase-stepped photoelastic data," *Exp. Mech.* **45**(3), 278–289 (2005).
27. J. Lesniak, S. J. Zhang, and E. A. Patterson, "Design and evaluation of the poleidoscope: a novel digital polariscope," *Exp. Mech.* **44**(2), 128–135 (2004).
28. D. R. Wolfson et al., "Rigid-body modelling of shaken baby syndrome," *J. Eng. Med.* **219**(1), 63–70 (2005).
29. R. A. Mrozek et al., "Polymer gels for defense applications," in *Mechanics of Biological Systems and Materials*, Vol. 7, Conference Proceedings of the Society for Experimental Mechanics Series 2015, pp. 47–51, Springer Science+Business Media, LLC, New York (2015).
30. Y. H. Zhao and J. Huang, "Photoviscoelastic stress analysis of a plate with a central hole," *Exp. Mech.* **41**(4), 312–318 (2001).
31. B. D. Coleman and E. H. Dill, "Theory of induced birefringence in materials with memory," *J. Mech. Phys. Solids* **19**, 215–243 (1971).
32. H. Weber, "Characterisation of photoviscoelastic materials by a non-linear constitutive equation," *Exp. Mech.* **27**(4), 390–397 (1987).
33. T. Spalton et al., "Streaming birefringence: a step forward," *Appl. Mech. Mater.* **13–14**, 23–28 (2008).

**Rachel A. Tomlinson** is a senior lecturer in mechanical engineering at the University of Sheffield. She gained a Bachelor of Engineering in mechanical engineering in 1991 and a PhD on the optical method of caustics, sponsored by British Aerospace, in 1995. Since then she has worked on a wide variety of research projects in the areas of fracture mechanics, digital image correlation, photoelasticity, tomographic photoelasticity, and thermoelastic stress analysis.

**Zeike A. Taylor** graduated in mechanical engineering from the University of Western Australia in 2002 and obtained his PhD in biomechanical engineering from the same institution in 2006. He has held postdoctoral fellowships at the CSIRO in Australia (2006), University College London (2007–2009), and the University of Queensland (2009–2011), and was an honorary lecturer at UCL in 2009. He joined the Department of Mechanical Engineering at the University of Sheffield as a lecturer in 2011.